Published by :
https://www.ijert.org/
An International Peer-Reviewed Journal

International Journal of Engineering Research & Technology (IJERT)
ISSN: 2278-0181
Vol. 15 Issue 03 , March - 2026

Removal of Sulfamethoxazole by Nano Zero-Valent Iron Loaded Yak Manure Biochar Prepared via Carbothermal Reduction

Haitao Yang,Yuxin Guo, Yurong Xie, Diancheng Zhang, Shiyuan Yang
College of Chemical and Environment
Southwest Minzu University
Chengdu, China

***Abstract*—Sulfamethoxazole (SMX) is a persistent sulfonamide antibiotic increasingly detected in Qinghai-Tibet Plateau water bodies, where low temperatures and intense UV irradiation retard its natural degradation. Although nano zero-valent iron (nZVI) can reduce and adsorb SMX, bare nZVI suffers from rapid aggregation and oxidation. In this study, yak manure biochar loaded with nZVI (Fe-YBC) was prepared by a one-step carbothermal reduction method at 900 °C, using $FeCl_3 \cdot 6H_2O$ as the iron precursor at a biomass-to-iron mass ratio of 5:1. Batch adsorption experiments showed that SMX removal by Fe-YBC followed pseudo-first-order kinetics ($R^2 = 0.984$) and the Langmuir isotherm model ($R^2 = 0.97$), indicating monolayer physisorption. The maximum adsorption capacity of Fe-YBC reached 193.54 mg/g at pH 3, approximately 2.6-fold higher than that of unmodified biochar (YBC, 73.34 mg/g). Adsorption efficiency decreased with increasing pH, consistent with the shift of SMX to its anionic form above pKa2 = 5.6. Coexisting cations inhibited adsorption in the order $Mg^{2+} > Ca^{2+} > K^+ > Na^+$, attributable to competitive site occupation modulated by ionic valence and hydrated radius. After five adsorption–desorption cycles using 75% ethanol as the desorbent, Fe-YBC retained over 86% of its initial removal efficiency. These findings suggest that carbothermal-reduction-derived Fe-YBC is a cost-effective and regenerable adsorbent for SMX removal and offers a route for valorizing yak manure waste in plateau regions.**

Keywords*—Sulfamethoxazole; Nano zero-valent iron; Yak manure biochar; Carbothermal reduction; Adsorption

I. INTRODUCTION

This template, Sulfonamide antibiotics are among the most widely prescribed antimicrobial agents in both human medicine and livestock husbandry [1,2]. Sulfamethoxazole (SMX), a broad-spectrum sulfonamide, is chemically stable, poorly biodegradable, and highly water-soluble, properties that favor its accumulation in surface water and groundwater rather than rapid attenuation [3]. Even at sub-milligram-per-liter concentrations, chronic SMX exposure induces oxidative stress and immunosuppression in aquatic organisms, and promotes the proliferation of antibiotic resistance genes (ARGs) in environmental microbial communities [4–6].

On the Qinghai-Tibet Plateau, the combination of low temperature, low dissolved oxygen, and intense seasonal UV produces an environment where antibiotic degradation rates are markedly lower than in lowland watercourses [7]. Recent surveys detected more than 40 antibiotic species in urban rivers of the northeastern Tibetan Plateau, with concentrations reaching up to several hundred ng/L; sulfonamide concentrations in certain tributaries exceeded internationally recognized environmental safety thresholds [7,8]. These data point to an urgent need for low-cost, locally adaptable adsorbents suited to plateau conditions.

Nano zero-valent iron (nZVI) has attracted attention for pollutant removal because of its large specific surface area and strong reductive capacity [9,10]. However, unsupported nZVI particles aggregate readily due to magnetic and van der Waals interactions, and oxidize on contact with air or water, which reduces the available reactive surface and shortens service life [11]. Loading nZVI onto porous carriers is therefore a common strategy to maintain particle dispersion and prolong reactivity [12].

Biochar, a carbonaceous solid produced by pyrolysis of biomass under oxygen-limited conditions, offers high porosity, large surface area, and chemical stability, making it a suitable carrier for nZVI [13]. Conventional preparation routes first pyrolyze biomass to obtain biochar, then impregnate it with iron salt, and finally reduce the iron to its zero-valent state using $NaBH_4$. This two-step process is both laborious and costly, and $NaBH_4$ introduces toxic by-products [14]. The carbothermal reduction method circumvents these drawbacks: during pyrolysis, reducing gases (CO, H_2) generated by the biomass itself convert Fe(III) or Fe(II) precursors to nZVI in a single heating step, yielding a composite material that retains the sorptive properties of biochar together with the reductive capacity of nZVI, without external chemical reductants [12,14].

On the eastern Qinghai-Tibet Plateau, yak dung is an abundant biomass resource whose disposal increasingly burdens grassland ecosystems as traditional energy consumption of dung declines [15]. Converting yak dung into a functional adsorbent for antibiotic removal would simultaneously address waste management and water quality objectives. In the present work, yak manure biochar loaded with nZVI (Fe-YBC) was prepared by one-step carbothermal reduction at 900 °C. Adsorption kinetics, isotherms, pH dependence, cation interference, and regeneration performance were systematically evaluated using SMX as the target pollutant, aiming to provide practical guidance for antibiotic pollution control in alpine regions.

International Journal of Engineering Research & Technology (IJERT)
ISSN: 2278-0181
Vol. 15 Issue 03 , March - 2026

II. EASE OF USE

A. Materials and Reagents

Yak dung was collected from a pasture at the Southwest Minzu University Ecological Protection and Animal Husbandry Research Base in Hongyuan County, Aba Tibetan and Qiang Autonomous Prefecture, Sichuan Province (32° 49′ N, 102° 34′ E, altitude ca. 3500 m). After air-drying, the dung was ground, crushed for 10 s in a biomass crusher (XA-3, Changzhou Xunsheng Instrument Co., Ltd., China), passed through a 60-mesh sieve, oven-dried at 80 °C for 24 h, and sealed for use. Sulfamethoxazole (SMX, $C_{10}H_{11}N_3O_3S$, purity 98%) was purchased from Shandong Keyuan Biochemical Co., Ltd. Ferric chloride hexahydrate ($FeCl_3·6H_2O$, AR), NaCl, KCl, $CaCl_2$, $MgCl_2$, KBr, HCl, and NaOH were all analytical-reagent grade.

B. Preparation of YBC and Fe-YBC

T For unmodified yak manure biochar (YBC), the pre-treated powder was loaded into a porcelain boat, compacted, and placed in a tube furnace (KJ-T1200-S80L1, Kejia Instrument, China). Under continuous N_2 flow, the furnace was heated from 25 °C to 900 °C at approximately 10 °C/min, held at 900 °C for 120 min, and then cooled naturally to room temperature. The resulting biochar was weighed and sealed for storage.

For nano-iron-loaded biochar (Fe-YBC), 9.65 g of $FeCl_3·6H_2O$ was dissolved in deionized water, and the solution was mixed with 10.00 g of pre-treated yak dung powder (biomass-to-Fe mass ratio = 5:1) [16]. The mixture was agitated on a shaker at 180 rpm for 30 min to ensure uniform impregnation, then dried at 70 °C for 24 h. The dried precursor was pyrolyzed under the same tube-furnace program described above for YBC. During pyrolysis, reducing gases (CO, H_2) generated by the biomass converted Fe(III) to nZVI in situ. The product was designated Fe-YBC.

C. Characterization

FTIR spectra were recorded on a Magna-IR 750 spectrometer (Nicolet, USA) over 400–4000 cm^{-1} at 1 cm^{-1} resolution with 32 scans, using KBr pellets (sample : KBr = 1 : 100, pressed at 10 MPa). Spectra of both materials were acquired before and after SMX adsorption to monitor changes in surface functional groups.

D. SMX Quantification

A 2 g/L SMX stock solution was prepared in 75% (v/v) ethanol. Standard solutions (0–25 mg/L) were measured at 261 nm on a UV-1800PC spectrophotometer (Shanghai Meipuda Instrument Co., Ltd., China), yielding a calibration equation y = 0.0629x + 0.0031 (R^2 = 0.9999). Because the present experiments used high-purity SMX dissolved in deionized water, interference from matrix ions was minimal; UV-Vis spectrophotometry was therefore adopted in place of HPLC.

E. Batch Adsorption Experiments

Kinetics. Adsorbent (0.04 g of YBC or Fe-YBC) was placed in 50 mL centrifuge tubes (triplicate) with 40 mL of 50 mg/L SMX solution. Tubes were shaken at 25 °C and 180 rpm. At designated time points (0.33, 0.67, 1, 2, 4, 6, 8, 10, 12, and 24 h), 10 mL aliquots were withdrawn, filtered through 0.45 μm membranes, diluted 1:1 with deionized water, and measured at 261 nm. Adsorption data were fitted to pseudo-first-order and pseudo-second-order kinetic models.

Isotherms. Fe-YBC (0.03 g) was contacted with 30 mL of SMX solution at initial concentrations of 25, 50, 75, 100, and 125 mg/L (triplicate) under the same shaking conditions for 24 h. Equilibrium data were fitted to the Langmuir and Freundlich isotherm models.

Effect of pH. YBC or Fe-YBC (0.04 g) was added to 40 mL of 50 mg/L SMX solution pre-adjusted to pH 3, 5, 7, 9, or 11 with HCl/NaOH (triplicate). After 24 h shaking at 25 °C, equilibrium concentrations were determined as above.

Effect of coexisting cations. To simulate plateau water chemistry, Na^+, K^+, Ca^{2+}, and Mg^{2+} were added individually at 50 mg/L—a concentration representative of most Qinghai-Tibet Plateau lakes and surface waters [17,18]—to 40 mL of 50 mg/L SMX solution containing 0.04 g adsorbent (triplicate, plus a cation-free control). Equilibrium concentrations were measured after 24 h.

Regeneration. Fe-YBC (0.04 g) was saturated with SMX as above, recovered by filtration, and desorbed in 40 mL of 75% (v/v) ethanol under the same shaking conditions for 24 h. The recovered material was dried at 70 °C to constant weight. Five consecutive adsorption–desorption cycles were performed, and removal efficiency was recorded for each cycle.

F. Batch Adsorption Experiments

The adsorption capacity q (mg/g) was calculated as $q = (C_0 - C_t) \times V \times k / m$, where C_0 and C_t are the initial and time-t SMX concentrations (mg/L), V is the solution volume (L), m is the adsorbent mass (g), and k is the dilution factor. Removal efficiency (%) = $(C_0 - C_t) / C_0 \times 100\%$. Kinetic data were fitted to the pseudo-first-order model ($q_t = q_e(1 - e^{(-k_1 t)})$) and the pseudo-second-order model ($q_t = q_e^2 k_2 t / (1 + q_e k_2 t)$). Equilibrium data were fitted to the Langmuir model ($q_e = q_{max} K_L Ce / (1 + K_L Ce)$) and the Freundlich model ($q_e = K_F Ce^{(1/n)}$).

III. RESULTS AND DISCUSSION

A. FTIR Analysis

FTIR spectra of YBC and Fe-YBC before and after SMX adsorption are presented in Figure 1. Both materials exhibited absorption bands corresponding to –OH stretching (3624 cm^{-1}), aliphatic C–H (2954 cm^{-1}), carbonyl C=O (1815 cm^{-1}), aromatic C=C (1550 cm^{-1}), C–O (1260 cm^{-1}), and Si–O (965 cm^{-1}). No new peaks appeared and no appreciable shifts occurred after adsorption, indicating that SMX removal was governed by physical interactions rather than covalent bond formation.

The limited involvement of nZVI in reductive degradation under these conditions may be attributed to the high biomass-to-iron ratio used during preparation: at 900 °C, the abundant carbonaceous matrix generated extensive porosity, and nZVI particles tended to distribute within the interior pore network of the biochar rather than on the external surface, thereby reducing their direct contact with SMX in solution [19].

International Journal of Engineering Research & Technology (IJERT)
ISSN: 2278-0181
Vol. 15 Issue 03 , March - 2026

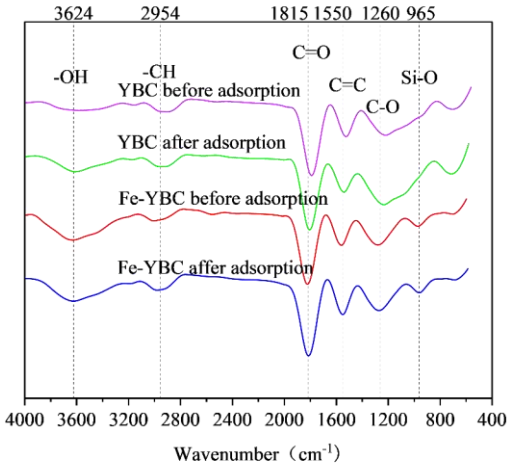

Figure 1. FTIR spectra of YBC and Fe-YBC before and after SMX adsorption.

.Adsorption Kinetics

The adsorption kinetics of YBC and Fe-YBC for SMX are shown in Figure 2, and the corresponding model parameters are listed in Table 1. Both materials reached approximate equilibrium within 4–6 h. The experimentally measured equilibrium adsorption capacities were 28.95 mg/g for YBC and 48.23 mg/g for Fe-YBC, closely matching the pseudo-first-order model predictions (28.005 and 46.263 mg/g, relative errors of 0.7% and 0.4%, respectively).

The pseudo-first-order model yielded higher R^2 values (0.972 for YBC; 0.984 for Fe-YBC) than the pseudo-second-order model (0.916 and 0.918), and the rate constants k_1 (0.090 and 0.072 min^{-1}) were substantially larger than k_2 (0.008 and 0.004 g/(mg·min)). These results indicate that physical diffusion between adsorbent and adsorbate, rather than surface chemical reaction, governed the adsorption rate, a conclusion consistent with the FTIR evidence described above.

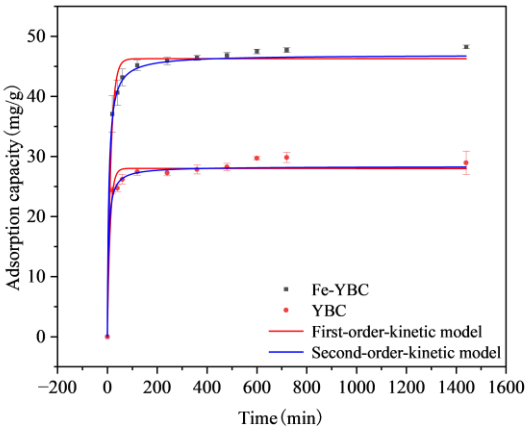

Figure 2. Adsorption kinetics fitting curves for YBC and Fe-YBC.

Table 1 Adsorption kinetic fitting parameters (pseudo-first-order left; pseudo-second-order right; k_2 unit: g/(mg·min)).

Sample	q_e (mg/g)	k_1 (1/min)	R^2	q_e (mg/g)	k_2	R^2	$q_{e,exp}$
YBC	28.005	0.090	0.972	28.323	0.008	0.916	28.95
Fe-YBC	46.263	0.072	0.984	46.902	0.004	0.918	48.23

B. Adsorption Isotherm

Isotherm fitting results for Fe-YBC at 25 °C are shown in Figure 3 and Table 2. The Langmuir model provided a higher correlation coefficient (R^2 = 0.97) than the Freundlich model (R^2 = 0.91), suggesting that SMX adsorption occurred on a finite number of equivalent sites in a monolayer configuration. The theoretical maximum adsorption capacities (q_m) derived from the Langmuir fit were 73.34 mg/g for YBC and 193.54 mg/g for Fe-YBC. The Freundlich parameter n exceeded unity for both materials (3.13 and 1.72), confirming that adsorption was energetically favorable under the tested conditions.

The 2.6-fold increase in q_m upon nZVI loading points to the role of the iron phase in expanding the adsorptive capacity of the composite. By comparison, Xu et al. [20] reported maximum SMX adsorption capacities for Fe–N co-doped biochar substantially lower than the 193.54 mg/g observed here, a difference that likely reflects variations in feedstock, pyrolysis temperature, and resulting surface properties.

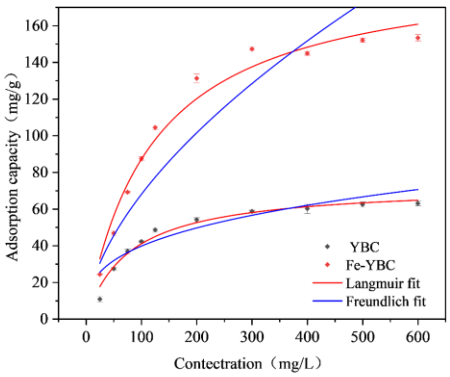

Figure 3. Adsorption isotherm fitting curves for YBC and Fe-YBC at 25 °C.

Table 2 Adsorption isotherm fitting parameters at 25 °C (Langmuir left; Freundlich right).

Sample	q_m (mg/g)	K_L (L/mg)	R^2	n	K^f (L/g)	R^2
YBC	73.34	0.01	0.97	3.13	9.09	0.86
Fe-YBC	193.54	0.01	0.97	1.72	4.730	0.91

C. Effect of Solution pH

The influence of initial pH on SMX adsorption is presented in Figure 4. Both YBC and Fe-YBC exhibited the

International Journal of Engineering Research & Technology (IJERT)
ISSN: 2278-0181
Vol. 15 Issue 03 , March - 2026

highest adsorption capacity at pH 3, with a progressive decline as pH increased to 11. SMX has two dissociation constants (pKa1 = 1.7, pKa2 = 5.6) [21]: below pKa1, the molecule carries a net positive charge; between pKa1 and pKa2, the neutral form dominates; above pKa2, the anionic species prevails. Because biochar surfaces are negatively charged over the tested pH range, electrostatic attraction between the protonated/neutral SMX and the biochar surface is strongest under acidic conditions, whereas electrostatic repulsion between anionic SMX and the negatively charged surface suppresses adsorption at pH 7–11.

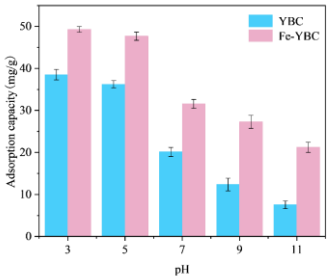

Figure 4. Effect of solution pH on SMX adsorption by YBC and Fe-YBC."

D. Effect of Coexisting Cations

The presence of 50 mg/L Na^+, K^+, Ca^{2+}, or Mg^{2+} all reduced SMX adsorption relative to the cation-free control (Figure 5). The degree of inhibition followed the order Mg^{2+} > Ca^{2+} > K^+ > Na^+. Divalent cations (Mg^{2+}, Ca^{2+}) carry higher charge density than monovalent species and thus compete more aggressively for negatively charged adsorption sites on the biochar surface. Between the two divalent cations, Mg^{2+} possesses a smaller hydrated ionic radius (4.28 Å vs. 4.12 Å for Ca^{2+}), allowing it to penetrate micropores more readily and occupy a greater fraction of the internal adsorption space. This competitive-site-occupation mechanism is consistent with the monolayer adsorption behavior indicated by the Langmuir isotherm fitting.

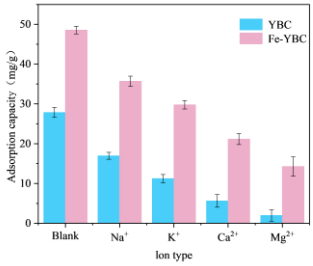

Figure 5. Influence of common cations in plateau water bodies on SMX adsorption efficiency.

E. Regeneration Performance

Over five consecutive adsorption–desorption cycles using 75% ethanol, the SMX removal efficiency of Fe-YBC decreased from an initial 98% to 86% (Figure 6). The gradual decline may result from incomplete desorption of SMX molecules bound at high-energy sites or from partial oxidation of nZVI during repeated wetting and drying. Nonetheless, retaining over 86% efficiency after five cycles confirms acceptable reusability for repeated field deployment.

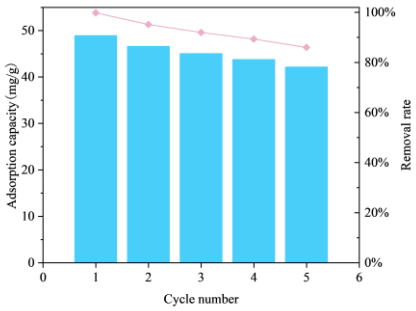

Figure 6. Effect of adsorption–desorption cycle number on SMX removal efficiency of Fe-YBC.

Table 3 compares the maximum SMX adsorption capacities of biochar derived from various feedstocks. YBC (73.34 mg/g) already exceeds the values reported for coffee grounds (0.13 mg/g) [22], pomelo peel (0.83 mg/g) [23], rice straw (1.83 mg/g) [24], reed (4.99 mg/g) [25], sewage sludge (5.43 mg/g) [26], pine sawdust (13.83 mg/g) [27], walnut wood (23.60 mg/g) [28], sugarcane bagasse (35.43 mg/g) [29], alfalfa (47.88 mg/g) [30], and traditional Chinese medicine residues (51.22 mg/g) [31]. After nZVI loading, Fe-YBC reached 193.54 mg/g, substantially exceeding all other feedstocks tested. The superior capacity of yak manure biochar may be attributed to its large specific surface area and well-developed pore structure formed during high-temperature pyrolysis, while the uniformly dispersed nZVI particles produced by carbothermal reduction contributed additional active sites.

***Table 3** Comparison of maximum SMX adsorption capacities of biochars from various feedstocks.*

Feedstock	*Pyrolysis T (°C)*	*q_{max} (mg/g)*	*Ref.*
Coffee grounds	*450*	*0.13*	*[22]*
Pomelo peel	*350*	*0.83*	*[23]*
Rice straw	*400*	*1.83*	*[24]*
Reed	*300*	*4.99*	*[25]*
Sewage sludge	*600*	*5.43*	*[26]*
Pine sawdust	*650*	*13.83*	*[27]*
Walnut wood	*450*	*23.60*	*[28]*

International Journal of Engineering Research & Technology (IJERT)
ISSN: 2278-0181
Vol. 15 Issue 03 , March - 2026

Sugarcane bagasse	*800*	*35.43*	*[29]*
Alfalfa	*800*	*47.88*	*[30]*
Chinese medicine residue	*750*	*51.22*	*[31]*
Yak manure (this study)	*900*	*73.34*	—
Yak manure + nZVI (this study)	*900*	*193.54*	—

IV. CONCLUSION

A yak manure biochar loaded with nano zero-valent iron (Fe-YBC) was prepared by one-step carbothermal reduction at 900 °C and evaluated for sulfamethoxazole (SMX) removal from aqueous solution. The key findings are summarized below.

Fe-YBC exhibited a maximum Langmuir adsorption capacity of 193.54 mg/g at pH 3, approximately 2.6 times higher than that of unmodified YBC (73.34 mg/g). Adsorption kinetics followed the pseudo-first-order model (R^2 = 0.984), and FTIR spectra showed no new functional-group peaks after adsorption, jointly indicating a physisorption-dominated process. Solution pH exerted a pronounced effect: adsorption capacity was highest under acidic conditions and declined progressively with increasing pH, consistent with the electrostatic interaction between anionic SMX (above pKa2 = 5.6) and the negatively charged biochar surface. Among the four plateau-relevant cations tested at 50 mg/L, Mg^{2+} caused the strongest inhibition, followed by Ca^{2+}, K^{+}, and Na^{+}, reflecting the combined influence of ionic charge density and hydrated radius on competitive site occupation. After five adsorption–desorption cycles, Fe-YBC retained over 86% of its initial removal efficiency, demonstrating acceptable regenerability.

Compared with biochars derived from ten other feedstocks, the yak manure-based materials ranked highest in SMX adsorption capacity under comparable conditions. These results indicate that the carbothermal reduction route provides a simple, reagent-free strategy for preparing nZVI-loaded biochar from plateau livestock waste, with potential relevance to antibiotic contamination control in alpine water bodies.

Several limitations should be noted. The present study relied on FTIR as the sole characterization technique; supplementary analyses such as SEM, BET surface area measurement, and XRD would help clarify the distribution of nZVI particles within the biochar matrix and its relationship to adsorption performance. The mechanism by which nZVI enhances adsorption capacity—whether through additional active sites, altered surface charge, or partial reductive transformation of SMX—remains to be elucidated. Future studies should incorporate multi-technique characterization and explore the co-removal behavior of Fe-YBC toward antibiotics and co-occurring pollutants under field-relevant conditions.

ACKNOWLEDGMENT

The authors thank the staff at the Hongyuan Ecological Protection and Animal Husbandry Research Base for providing yak dung samples.

REFERENCES

[1] Chafer-Pericas, C., Maquieira, A., Puchades, R., et al. (2011). Multiresidue determination of antibiotics in feed and fish samples for food safety evaluation. Food Control, 22(6), 993–996.

[2] Yang, Q., Zhang, H., Guo, Y., et al. (2016). Influence of chicken manure fertilization on antibiotic-resistant bacteria in soil and the endophytic bacteria of pakchoi. Int. J. Environ. Res. Public Health, 13(7), 662.

[3] Prasannamedha, G., & Senthil Kumar, P. (2020). A review on contamination and removal of sulfamethoxazole from aqueous solution using cleaner techniques: Present and future perspective. J. Clean. Prod., 250, 119553.

[4] Zhu, Y.-G., Zhao, Y., Li, B., et al. (2017). Continental-scale pollution of estuaries with antibiotic resistance genes. Nature Microbiology, 2, 16270.

[5] Qiu, W., Liu, X., Yang, F., et al. (2020). Single and joint toxic effects of four antibiotics on some metabolic pathways of zebrafish larvae. Sci. Total Environ., 716, 137062.

[6] Xing, Z., Li, H., Li, M., et al. (2021). Disequilibrium in chicken gut microflora with avian colibacillosis is related to microenvironment damaged by antibiotics. Sci. Total Environ., 762, 143058.

[7] Kuang, Y., Guo, X., Hu, J., et al. (2020). Occurrence and risks of antibiotics in an urban river in northeastern Tibetan Plateau. Sci. Rep., 10, 20054.

[8] Zhang, Q.-Q., Ying, G.-G., Pan, C.-G., et al. (2015). Comprehensive evaluation of antibiotics emission and fate in the river basins of China: Source analysis, multimedia modeling, and linkage to bacterial resistance. Environ. Sci. Technol., 49(11), 6772–6782.

[9] Penrose, W. R., & Woolson, E.-A. (1974). Arsenic in the marine and aquatic environments: Analysis, occurrence, and significance. Crit. Rev. Environ. Sci. Technol., 4(4), 465–482.

[10] Li, J., Zhou, Q., Liu, Y., et al. (2017). Recyclable nanoscale zero-valent iron-based magnetic polydopamine coated nanomaterials for the adsorption and removal of phenanthrene and anthracene. Sci. Technol. Adv. Mater., 18(1), 3–16.

[11] Shaheen, S. M., Mosa, A., Natasha, et al. (2022). Removal of toxic elements from aqueous environments using nano zero-valent iron- and iron oxide-modified biochar: A review. Biochar, 4, Article 24.

International Journal of Engineering Research & Technology (IJERT)
ISSN: 2278-0181
Vol. 15 Issue 03 , March - 2026

[12] Li, S., You, T., Guo, Y., et al. (2019). High dispersions of nano zero valent iron supported on biochar by one-step carbothermal synthesis and its application in chromate removal. RSC Adv., 9(22), 12428–12435.

[13] Wang, S., Zhao, M., Zhou, M., et al. (2019). Biochar-supported nZVI (nZVI/BC) for contaminant removal from soil and water: A critical review. J. Hazard. Mater., 373, 820–834.

[14] Nisticò, R., & Carlos, L. (2019). High yield of nano zero-valent iron (nZVI) from carbothermal synthesis using lignin-derived substances from municipal biowaste. J. Anal. Appl. Pyrolysis, 140, 239–244.

[15] Yang, Y., Liu, G., Ye, C., et al. (2019). Bacterial community and climate change implication affected the diversity and abundance of antibiotic resistance genes in wetlands on the Qinghai-Tibetan Plateau. J. Hazard. Mater., 361, 283–293.

[16] Liu, Y., Sohi, S.-P., Liu, S., et al. (2019). Adsorption and reductive degradation of Cr(VI) and TCE by a simply synthesized zero valent iron magnetic biochar. J. Environ. Manage., 235, 276–281.

[17] Sun, M., Jin, H., Yao, X., et al. (2020). Hydrochemistry differences and causes of tectonic lakes and glacial lakes in Tibetan Plateau. Water, 12(11), 3165.

[18] Qu, B., Zhang, Y., Kang, S., & Sillanpää, M. (2019). Water quality in the Tibetan Plateau: Major ions and trace elements in rivers of the “Water Tower of Asia.” Sci. Total Environ., 649, 571–581.

[19] Duan, C., Ren, J., Tao, L., et al. (2023). Study of the remediation effect and mechanism of biochar-loaded nZVI on heavy metal contaminated soil. Sustainability, 15(24), 16753.

[20] Xu, L., Wu, C., Chai, C., et al. (2022). Adsorption of micropollutants from wastewater using iron and nitrogen co-doped biochar: Performance, kinetics and mechanism studies. J. Hazard. Mater., 424(Part C), 127606.

[21] Lucida, H., Parkin, J. E., & Sunderland, V. B. (2000). Kinetic study of the reaction of sulfamethoxazole and glucose under acidic conditions: I. Effect of pH and temperature. Int. J. Pharm., 202(1–2), 57–62.

[22] Zhang, X., Zhang, Y., Ngo, H., et al. (2020). Characterization and sulfonamide antibiotics adsorption capacity of spent coffee grounds based biochar and hydrochar. Sci. Total Environ., 716, 137015.

[23] Cheng, D., Ngo, H., Guo, W., et al. (2020). Applying a new pomelo peel derived biochar in microbial fuel cell for enhancing sulfonamide antibiotics removal in swine wastewater. Bioresour. Technol., 318, 124070.

[24] Han, X., Liang, C.-F., Li, T.-Q., et al. (2013). Simultaneous removal of cadmium and sulfamethoxazole from aqueous solution by rice straw biochar. J. Zhejiang Univ. Sci. B, 14(7), 640–649.

[25] Zheng, H., Wang, Z., Zhao, J., et al. (2013). Sorption of antibiotic sulfamethoxazole varies with biochars produced at different temperatures. Environ. Pollut., 181, 60–67.

[26] Ma, Y., Yang, L., Wu, L., et al. (2020). Carbon nanotube supported sludge biochar as an efficient adsorbent for low concentrations of sulfamethoxazole removal. Sci. Total Environ., 718, 137263.

[27] Reguyal, F., Sarmah, A. K., & Gao, W. (2017). Synthesis of magnetic biochar from pine sawdust via oxidative hydrolysis of $FeCl_2$ for the removal of sulfamethoxazole from aqueous solution. J. Hazard. Mater., 321, 868–878.

[28] Huang, J., Zimmerman, A. R., Chen, H., et al. (2020). Ball milled biochar effectively removes sulfamethoxazole and sulfapyridine antibiotics from water and wastewater. Environ. Pollut., 258, 113809.

[29] Zhang, R., Zheng, X., Chen, B., et al. (2020). Enhanced adsorption of sulfamethoxazole from aqueous solution by Fe-impregnated graphited biochar. J. Clean. Prod., 256, 120662.

[30] Li, Q., Yu, W., Guo, L., et al. (2021). Sorption of sulfamethoxazole on inorganic acid solution-etched biochar derived from alfalfa. Materials, 14(4), 1033.

[31] Deng, J., Li, X., Wei, X., et al. (2020). Hybrid silicate-hydrochar composite for highly efficient removal of heavy metal and antibiotics: Coadsorption and mechanism. Chem. Eng. J., 387, 124097.